Assigning a structural motif using spontaneous molecular dipole orientation in thin films†

M. Roman, [ID] [a] A. Dunn,‡[a] S. Taj,[a] Z. G. Keolopile,[ab] A. Rosu-Finsen, [ID] §[a] M. Gutowski, [ID] [a] M. R. S. McCoustra, [ID] *[a] A. M. Cassidy [ID] [c] and D. Field [ID] [c]

Spontaneous orientation of molecular dipoles has been observed to produce bulk electric fields, termed 'spontelectric' fields, in a broad variety of molecular solid thin films formed by condensation from the gas phase. Such spontelectric fields are found in *cis*-methyl formate (*cis*-MF) and the present work combines observation of these fields with high quality *ab initio* studies of *cis*-MF monomers and dimers. This enables a prediction of the structural motif within the unit cell of the crystalline phase of solid *cis*-MF, showing it to be a non-polar dimer. Dimer formation at deposition temperatures of >90 K is therefore cited to contribute to the observed collapse of the spontelectric field at these temperatures. This is the first time that such a structural prediction has been made using observations of spontelectric behaviour as a key indicator.

Introduction

Powerful electric fields form in vapour deposited films of polar molecules and are the result of spontaneous orientation of the dipoles of the molecules involved.[1–5] The extent of dipole orientation, giving rise to this so-called 'spontelectric effect', has been described by an interplay between intermolecular forces, the electric field present in the material and the tendency to disorder introduced through thermal motion. This represents a classic order–disorder system. Here, we introduce a new element into our understanding of the spontelectric phenomenon, suggesting that, as the temperature of deposition of films is raised, new structural motifs may arise which are themselves non-polar. Thus, the collapse of the spontelectric field at higher deposition temperatures may be viewed, in the case of *cis*-methyl formate (*cis*-MF) at a Curie temperature of >90 K, not only as a manifestation of competition between order and disorder, but also one in which new order additionally precludes the formation of the spontelectric state through the formation of non-polar structures.

The following salient observational properties of materials exhibiting such spontaneous dipole orientation have been identified so far[3–5] by Field and co-workers:

(i) Surface potentials at the vacuum/film interface may be positive or negative.

(ii) The spontelectric field depends on the temperature at which the film is deposited.

(iii) Heating a spontelectric film reveals a Curie temperature, at which the spontelectric effect decays abruptly. Subsequent cooling to below the Curie point has not been observed to reintroduce a surface potential.

(iv) The nature of the surface, upon which spontelectric films are deposited, has essentially no bearing on the values of surface potential.

(v) If the parent gas is diluted in a non-dipolar gas, a decrease is observed in the spontelectric field, to zero at sufficient dilution.

(vi) Spontelectric films may undergo a phase change whilst preserving their spontelectric character.

Field and co-workers were able to develop a simple para-meterized order–disorder analysis explaining the resulting spontelectric fields, in films of materials deposited from vacuum, in terms of the temperature-dependent degree of dipole orientation in the solid material,[3–5] verifying Kutzner's original supposition.[1] Combining this analysis with experimental results for about a dozen small species of disparate structure, ranging from CO to methyl formate to toluene, the spontelectric effect has been shown to be both non-local and non-linear. The non-linearity inherent in spontelectrics, see below, is best illustrated by studies of *cis*-MF,[6,7] the subject of the present work.

[a] *Institute of Chemical Sciences, Heriot-Watt University, Edinburgh, EH14 4AS, UK. E-mail: m.r.s.mccoustra@hw.ac.uk*

[b] *Department of Physics, University of Botswana, Private Bag 0022, Gaborone, Botswana*

[c] *Department of Physics and Astronomy, University of Aarhus, Aarhus, DK-8000, Denmark*

† Electronic supplementary information (ESI) available. See DOI: 10.1039/c8cp06010j

‡ Current address: Q2 Solutions, Alba Campus, Rosebank, Livingston, West Lothian, EH54 7EG, UK.

§ Current address: Department of Chemistry, University College London, London, WC1H 0AJ, UK.

Exploration of the spontelectric nature of N_2O allowed identification of the impact of the vibrational Stark effect on LO–TO splitting of molecular vibrations in thin solid films as an alternative means of identifying spontelectric materials[8] and demonstrated the potential of neutron scattering as a structural probe of the spontelectric phase.[9] With a simple infrared spectroscopic characterisation method available, the spontelectric nature of carbon monoxide thin films was also demonstrated.[10] This in turn furnished an explanation for the longstanding problem in the electronic spectroscopy of solid CO,[11] and other species (*e.g.* ammonia[12]), of substantial band origin shifts with deposition temperature through the impact of the electronic Stark effect on Wannier–Mott excitons within a spontelectric solid. The impact of the spontelectric effect on star formation and its potential for engineering electric field structures has also been explored.[3–5] In addition, the impetus of the substantial body of work by Field and co-workers [ref. 3–5 and references therein] has prompted others into investigating this novel, electrical phase of molecular materials.[13,14]

However, while we have made substantial strides in characterising molecular solids exhibiting spontelectric behaviour, we have as yet to identify more precisely the molecular motifs and balance of intermolecular interactions that necessarily drive this non-linear and non-local phenomenon. Evidence does, however, point to the observation that systems exhibiting strong hydrogen bond interactions may not behave spontelectrically where the directionality of the hydrogen bond dominates. Water nicely illustrates this, with observations from Field and co-workers that highlight the absence of spontelectric behaviour in amorphous solid water at deposition temperatures above 40 K[15] while results in Bu *et al.*[13] suggest that lower deposition temperatures, where the hydrogen bond connectivity is significantly reduced, result in a material which essentially behaves spontelectrically. The observations on butan-1-ol[14] would support this. Within the body of work by Field and co-workers, *cis*-MF and ethyl formate are representative of species which behave spontelectrically and reveal weak hydrogen bond interactions *via* the formate ester motif.[3–5,12,13] *cis*-MF also exhibits unusual spontelectric behaviour in that the measured spontelectric field is first observed to decrease as deposition temperature is increased up to 77 K in the normal manner; but above 77 K is then observed to increase before the spontelectric field disappears completely above 90 K. This counter-intuitive, non-linear behaviour was predicted by the model of Field *et al.* and serves as a powerful indicator that this model captures some of the essential physics of the spontelectric effect. The mathematical form of the spontelectric model reproduces the anomalous data for *cis*-MF in which the degree of dipole orientation increases at deposition temperatures > 77 K. However, only a qualitative physical explanation is presently available for this behaviour, which appears at first sight to contradict a simple order–disorder model.[3] A detailed infrared (IR) study of *cis*-MF has also revealed this bi-modal behaviour with temperature below and above 77 K and is entirely consistent with the non-linear and non-local growth of spontelectric materials.[7]

For completeness, we should also note that dipole orientation has also been identified in organic light-emitting diode materials [ref. 16 and references therein]. Such films have electrical properties quite distinct from those of spontelectrics. Partial ordering, in these cases of large organics, may be based on local non-bonded interactions of the molecules with the substrate, rather than on the dipole–dipole interactions.[17] In this connection, the spontelectric phenomenon is also quite distinct from the ferroelectric effect, as discussed at length in ref. 3.

The current work complements the work reported in ref. 7 and demonstrates, for the first time, the clear potential of spontelectric measurements in helping to reveal the structural motif inherent in a solid phase. While the IR spectroscopy of thin films of MF is relatively well known,[18,19] the absence of any structural data has made interpretation of the spectra as a function of deposition temperature more complex. In this paper, we will demonstrate how knowledge of the spontelectric behaviour of MF, in particular the collapse of the spontelectric phenomenon at deposition temperatures > 90 K, can directly inform on the structure of the solid state.

Experimental and computational methodology

Reflection–absorption IR (RAIR) spectra of MF in the spectral range 700 to 4000 cm^{-1} were obtained at Heriot-Watt University using essentially the same method as reported for N_2O[2] and are reported in detail in ref. 7.

The experiments were conducted in an ultrahigh vacuum (UHV) chamber equipped with a line-of-sight quadrupole mass spectrometer (QMS, Hiden Analytical, HAL 3F/PIC) and a Fourier-transform infrared spectrometer (Varian 670-IR) configured for RAIR spectroscopy, at a grazing angle incidence of 75° with respect to the normal to the substrate. After reflection from the sample, the IR beam was focused onto a liquid nitrogen cooled HgCdTe detector. The base temperature of the system, achieved using a closed-cycle helium refrigerator (APD Cryogenics, HC-2), was 18 K as measured using a KP-type thermocouple. The substrate for MF film growth was oxygen-free, high conductivity copper, coated with a 250 nm layer of amorphous silica. The presence of amorphous silica allows the detection of TO modes[2] and spectra, taken at a resolution of 0.1 cm^{-1}, hence show LO–TO splitting, key for the analysis involving the spontelectric effect. Spectral splitting is referred to throughout as LO–TO splitting, whilst recognizing that the absolute value of the splitting arises through a combination of the intrinsically different vibrational frequencies associated with LO and TO modes and a contribution due to the vibrational Stark effect.

Liquid phase IR spectra were recorded using the attenuated total reflectance (ATR) technique on a Thermo Nicolet iS5 FTIR spectrometer fitted with an iD7 ATR accessory. The spectrum reported results from the co-addition of 16 spectral scans at a resolution of 1 cm^{-1}. This gives us a set of IR spectra unperturbed by the effects of the solid state for comparison.

We recognize that the absolute energies of the individual molecules and that of the dimers (see below) will be affected by the presence of other surrounding species in the solid state. However, viewing this influence as a uniform perturbation which permeates the medium in a simple isotropic manner, we make the assumption here that the differences between the energies of the monomer and the dimers in the solid state may be represented by the differences for isolated species, as calculated here. On this basis, isolated MF was subject to investigation by electronic structure calculations at the coupled cluster level of theory[20] with single and double excitations (CCSD/aug-cc-pVTZ (ATZ)[21,22]) in geometry optimizations and harmonic frequency calculations, and additional non-iterative triple excitations (CCSD(T)) in single-point energy calculations. The SCF and MP2 energies were extrapolated to the basis set limit.[23] The dipole moments were calculated with the CCSD/ATZ densities. Finally, anharmonic corrections to vibrational frequencies were calculated at the MP2/ATZ level.[24]

The MF monomer is equipped with a strong proton acceptor, but it lacks a strong proton donor. We expect the MF dimers to be only weakly bound, and therefore computational results might be contaminated with basis set superposition errors. Thus the geometries and harmonic frequencies of MF dimers were characterized on the counterpoise-corrected potential energy surface at the MP2/aug-cc-pVDZ (ADZ)[21,22] level. We have considered 43 initial orientations of the monomers, including *cis–cis*, *cis–trans*, and *trans–trans* complexes. As proton donors, we have considered both the CH_3 and CH hydrogens, and as proton acceptors both the carbonyl and ester oxygens. The geometry optimizations initiated from these 43 initial structures converged to 16 structures shown in the ESI,† Fig. S1. The *cis–cis* and *trans–trans* complexes were the most and least stable, respectively. Thus the *cis–cis* complexes were studied more thoroughly. The total stabilization energy of the dimer was calculated as a sum of two one-body terms (repulsive terms resulting from deformations of the monomers in the dimer) and an attractive two-body term (the interaction energy between two deformed monomers), see ref. 25.
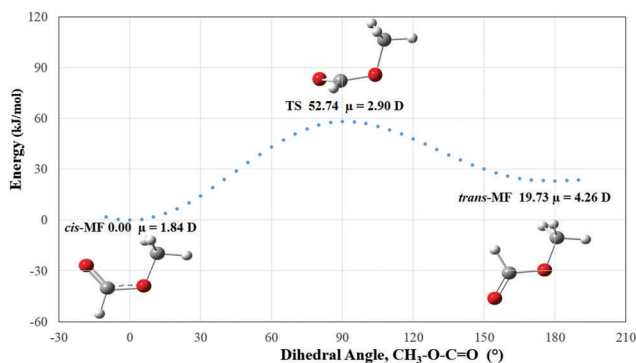

Fig. 1 Electronic energy profile for methyl formate (MF) along the dihedral CH_3–O–C=O angle. Three stationary points are illustrated: *cis*-MF, transition state TS, and *trans*-MF, with the energies corrected for zero-point vibrations. The dipole moment increases from *cis*-MF through the TS to *trans*-MF. The experimental dipole moment of *cis*-MF is 1.77 D.[27]

Results and discussion

Methyl formate rotational isomerism in the gas phase

MF is subject to rotational isomerism around both the methyl–oxygen and the formyl–oxygen bonds, *i.e.* the dihedral angles H–CH_2–O–C and CH_3–O–C=O. Internal rotation about the latter is the most significant with electronic structure results shown in Fig. 1 indicating that *cis*-MF is 19.7 kJ mol^{-1} more stable than *trans*-MF with a separating barrier of 52.7 kJ mol^{-1}. The polarity increases from *cis*-MF to *trans*-MF, 1.84 D and 4.26 D, respectively. The geometries of these three stationary points are tabulated in the ESI,† Table S1.

The MP2 and CCSD harmonic vibrational constants and MP2 anharmonic corrections for the 0–1 transition for *cis*-MF, *trans*-MF, and the transition state are tabulated in the ESI,† Tables S2–S4, whereas here we focus on the C=O stretching mode only, which has the highest intensity in the *cis*- and *trans*-MF species. The calculated CCSD harmonic vibrational constant is 1827 and 1869 cm^{-1} and the 0–1 anharmonic transition is predicted at 1796 and 1841 cm^{-1} for the gas phase

Table 1 Harmonic (H) C=O vibrational constant, anharmonic (AH) correction to the 0–1 transition, and anharmonic 0–1 transition (cm^{-1}) in *cis*- and *trans*-MF. δMP2(AH) stands for anharmonic correction obtained at the MP2 level. All results obtained with the ATZ basis set

	C=O vibrational mode				
Structure	CCSD(H)	MP2(H)	MP2(AH)	δMP2(AH)	CCSD(H) + δMP2(AH)
cis	1827.0	1769.5	1738.5	−31.0	1796.0
trans	1869.1	1807.1	1778.5	−28.5	1840.6

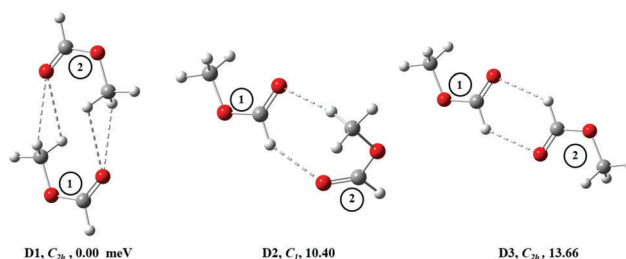D1, C_{2h}, 0.00 meV   D2, C_1, 10.40   D3, C_{2h}, 13.66

Fig. 2 The three most stable dimers of MF, with the monomers labelled as **1** and **2** (see Table 2). The relative energies are given in meV.

Table 2 Total stabilisation energy in the D1–D3 dimers represented as a sum of one-body components (monomer deformation terms), two-body interaction energy between deformed monomers, and a zero-point vibration energy contribution (all terms in meV). The monomers **1** and **2** in each Dn, *e.g.*, **1@D1**, are specified in Fig. 2

Dimer	Monomer	$E_{cis\text{-MF}}^{1b\text{-def}}$	$E_{1\leftrightarrow 2}^{2b}$	$E_{1\leftrightarrow 2}^{Stab}$	ΔE_0^{vib}	$E_{1\leftrightarrow 2}^{Stab} + \Delta E_0^{vib}$
D1	**1@D1**	2.30	−199.03	−194.43	25.47	−168.96
	2@D1	2.30				
D2	**1@D2**	4.64	−194.47	−185.95	27.40	−158.56
	2@D2	3.88				
D3	**1@D3**	4.65	−182.93	−173.63	18.34	−155.30
	2@D3	4.65				

29040 | *Phys. Chem. Chem. Phys.*, 2018, **20**, 29038–29044
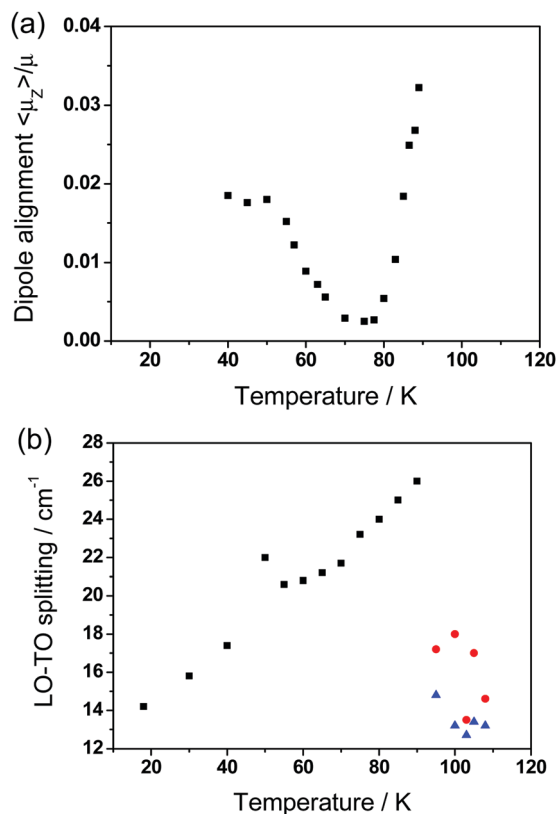
This journal is © the Owner Societies 2018

Fig. 3 (a) The variation of the degree of dipole alignment, $\langle\mu_z\rangle/\mu$, as a function of deposition temperature for the *cis*-MF film resulting from a 2000 L (1 L $\equiv$ 10^{-6} mbar s) exposure to MF vapour at room temperature; (b) variation of LO–TO splitting, $\Delta_{\text{LO–TO}}$, as a function of deposition temperature for an equivalent film of *cis*-MF where the black squares represent the splitting for a single C=O mode as observed in the amorphous phase of *cis*-MF and the red circles/blue triangles represent the pair of C=O stretching modes observed in the crystalline phase.

cis- and *trans*-MF, respectively, see Table 1. The results for *cis*-MF are in good agreement with the experimental gas phase spectrum.[26]

Simple Boltzmann analysis then suggests the *trans*-form comprises significantly less than 1 part in 10^8 of the total in the gas phase up to 120 K. In view of a high barrier separating *cis* from *trans*, and weak intermolecular interactions between MF molecules reflected by the melting point of MF of 173 K,

we assume that the spontelectric measurements and IR spectroscopy exclusively probe *cis*-MF in thin films.

Dimers of methyl formate

Sixteen low-energy structures of the MF dimer (D1–D16) are illustrated in the ESI,† Fig. S1. In view of the weakness of the intermolecular interactions, the relative energies and stabilization energies are given in meV (1 meV = 0.0965 kJ mol^{-1}). The results confirm that the carbonyl oxygen is a stronger proton acceptor than the ester oxygen. There are only minor stability preferences for the dimers, with proton donors resulting from CH_3 rather than from CH. The eight most stable dimers are assembled from two *cis*-monomers. The lowest energy dimer involving at least one *trans*-monomer, D9, is less stable than D1 by 182 meV (=17.6 kJ mol^{-1}).

Hereafter, we focus on the three most stable dimers of MF, D1–D3, illustrated in Fig. 2. Other dimeric structures are less stable by at least 30 meV at the MP2/ADZ level. Both D1 and D3 are symmetric (C_{2h}) and the small difference in stability (14 meV) results from a difference in the nature of the proton donors: CH_3 and CH, respectively. Not surprisingly, D2 has one CH_3 and one CH proton donor and its stability is in between D1 and D3, still 10 meV less stable than D1. D1 and D3 have overall zero dipole moments by symmetry, while the MP2 dipole moment of D2 is 0.75 D at the MP2/ADZ level. The total stabilization energies in D1–D3 are dominated by attractive two-body components (from −199 to −183 meV), with repulsive one-body deformation components for the *cis*-monomers not exceeding 5 meV, see Table 2. The zero-point vibrational corrections are destabilizing for all three dimers (between 18 and 27 meV), in agreement with our previous discussion.[25] Due to the weak hydrogen bonding, the C=O stretching modes are red-shifted in comparison with the isolated monomer; see Table S5 in the ESI.† The shift is more substantial for the symmetric than for the asymmetric C=O stretching mode. The asymmetric and symmetric modes become split by 10, 14, and 13 cm^{-1} in D1, D2, D3, respectively.

Spontelectric measurements on *cis*-MF thin films

Fig. 3(a) shows the variation of spontelectric field in *cis*-MF thin films as a function of deposition temperature taken from ref. 3–7.

Table 3 Comparison of the vibrational assignment of the IR spectrum of solid *cis*-MF from this work and from that of Palumbo and co-workers[18] and Brown and co-workers.[19] The amorphous *cis*-MF films were deposited at 16 K,[18] 26 K[19] and at 18 K in this work. Spectra of crystalline *cis*-MF were deposited at 110 K,[18] 105 K[19] and 108 K in this work

Vibration	Amorphous *cis*-MF peak positions			Crystalline *cis*-MF peak positions		
	18	19	This work	18	19	This work
CH_3 stretch	3038, 3010	3015	3011		3013, 3019	3012
CH stretch	2960	2964	2959		2963, 2978	2961, 1976
C=O stretch	1720	1736	1734, 1720	1713, 1707	1724, 1706	1717, 1706, 1710, 1697
CH_3 deformation	1450, 1453	1450, 1460	1453	1450, 1453	1440, 1451, 1459, 1472	1440, 1454, 1460
CH bend	1383	1388	1389		1394	1392
C–O stretch	1210	1228	1212	1210	1214, 1234	1213
CH_3 rock	1164	1173	1171	1164	1164, 1177	1166, 1173
O–CH_3 stretch	910	910	913	910	901, 906	899, 905
OCO deformation	768		769	768		770, 776

The highly anomalous behaviour expressed in this system of the degree of dipole orientation, and hence the spontelectric field, first decreasing with increasing deposition temperature then increasing as the temperature increases above 77 K is clearly observed. Explanation of this phenomenon in the context of non-linear and non-local growth of the spontelectric field in *cis*-MF films has been given in ref. 7. In the current work, we focus on the observation that above 90 K, no spontelectric field can be measured. Within the framework presented by Field and co-workers to explain the origin of spontelectric behaviour,[3–5] this can be interpreted as meaning that either the molecular dipoles are completely randomly oriented in an amorphous solid phase, due to thermal agitation, or alternatively, that 90 K represents a phase transition point and the crystalline solid phase prepared by deposition above 90 K presents a lattice motif in which the molecular dipoles are in a centrosymmetric structure.

Infrared spectroscopy of *cis*-MF thin films

Table 3 summarises our assignment of the IR spectrum of *cis*-MF in comparison to the reported work in ref. 18 and 19. A sharpening of the C=O line profile at around 1720 cm^{-1}, and of those of the other vibrational modes, is observed between 90 and 100 K. This is consistent with previous work from the literature[18,19] and suggests that at the higher deposition temperatures, the resulting film is crystalline in nature.

Fig. 4 presents experimental data recorded for films deposited at 70, 90 and 108 K to illustrate this behaviour and our analysis of LO–TO splitting of the C=O stretching mode, where the LO modes is observed to lie between 1733.8 and 1736.8 cm^{-1} while the TO modes lie between 1710.8 and 1713.2 cm^{-1}. Fig. 3(b) summarises the corresponding LO–TO splitting, Δ_{LO-TO}, as a function of deposition temperature.

In the amorphous phase (<90 K), a single LO–TO pair is observed. In the crystalline phase (>90 K), additional features consistent with a second LO–TO pair are observed. Comparing Fig. 3(a) and (b), we can see immediately that, below 90 K, are changes in the LO–TO splitting that are correlated to the presence of a spontelectric field. This can be successfully explained by the vibrational Stark effect.[7] Above 90 K, however, the absence of a spontelectric field means that the vibrational Stark Effect is switched off and the LO–TO splitting remains constant. Indeed, both LO–TO pairs observed in the crystalline phase at these temperatures show constant splitting as the temperature is increased beyond the crystallisation point.

Fig. 5 compares the crystalline phase C=O stretching features from previous reports on this system[18,19] with that of the current study. The liquid phase spectrum lacks any fine structure and illustrates the situation of truly randomly orientated dipoles. The RAIR spectrum from Brown and co-workers[19] (blue) reports measurements made on a graphite substrate and therefore subject to the metal surface selection rule. Consequently only the LO mode of the LO–TO split pair is observed. The RAIR spectra recorded in this work (black) and the transmission spectra of Palumbo and co-workers[18] (red) are remarkably similar in showing both components of the LO–TO splitting of the C=O stretching mode. This illustrates the fortuitous
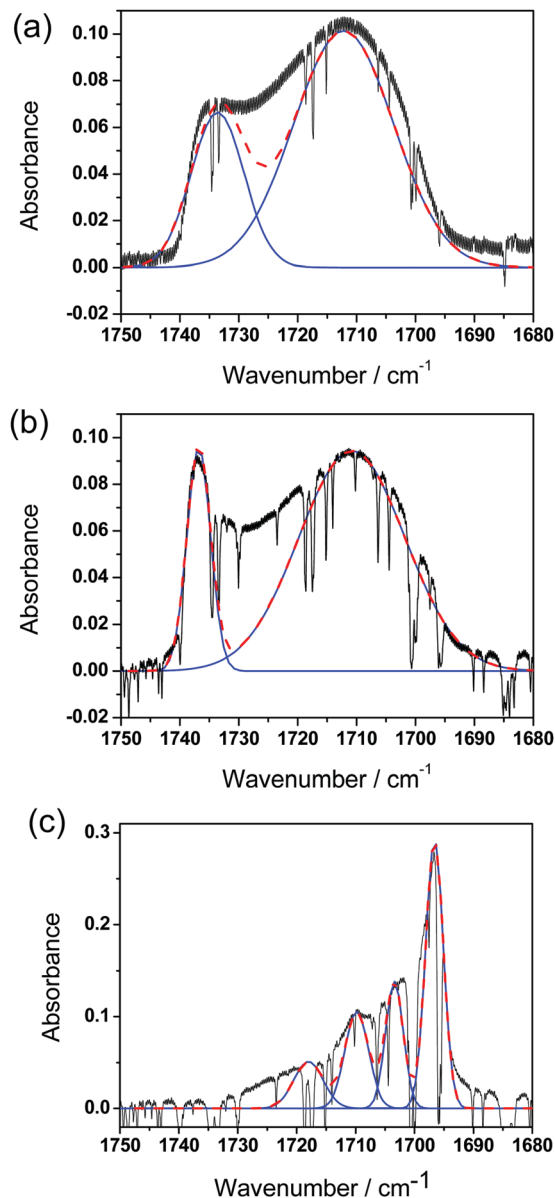

Fig. 4 RAIR spectra of solid *cis*-MF deposited on an amorphous silica film on a copper surface (black lines) for films of few 10's of ML. The sharp spectral features, useful as wavelength markers, are due to residual water vapour in the purge gas of our external optics. Spectrum (a) was recorded at 70 K deposition temperature, spectrum (b) was obtained at 90 K and spectrum (c) at 108 K. Spectra are the result of co-adding 512 scans at a resolution of 0.1 cm^{-1} in typically 60 minutes. The blue lines are Gaussian component fits to the LO and TO modes. As can be seen, the spectrum obtained at 108 K requires fitting with an additional two components compared to those at 70 and 90 K. The corresponding LO–TO splitting as a function of deposition temperature are shown in Fig. 3(b). The red dashed line shows the sum of the fits, the greater discrepancy at 90 K compared with 70 K indicating increasingly disordered molecular structure at higher deposition temperature.

advantage conferred, in the present study, of the 200 nm silica nanoparticulate film present on the copper substrate surface in allowing us to circumvent the metal surface selection rule.

So how do we explain both the additional LO–TO pair and the absence of a spontelectric field in the crystalline phase?
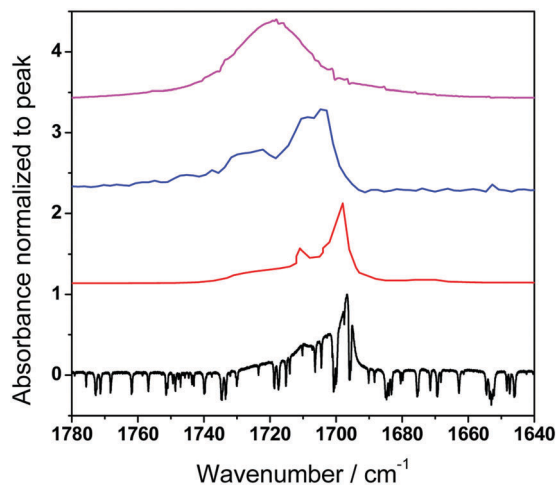
Fig. 5 The C=O stretching band of liquid (purple) and crystalline *cis*-MF from the present RAIRS study (black) and previously reported transmission studies by Palumbo and co-workers[18] (red) and RAIRS studies from Brown and co-workers[19] (blue). The narrow features in the black spectrum are a result of variation of the gas phase water content in dry air used to purge the external optics attached to the spectrometer and UHV system. Fig. 4(c) illustrates how even with the strong, but narrow, water features the black spectrum can be fitted to four components corresponding to the in-phase and out-of-phase LO–TO split C=O stretching mode.

We know that we are not observing the presence of both *cis*- and *trans*-rotational isomers in the crystalline phase. Comparison of the computed anharmonic frequencies in Table 1 with the observed frequencies in the crystalline phase clearly reveals that the shift between *cis*- and *trans*-isomer C=O stretching modes, at around 45 cm^{-1}, is substantially more than we observe in the experimental spectra. Hence, we can conclude that the additional LO–TO pair is unlikely to be associated with the presence of *trans*-MF.

Our hypothesis is that the neighbouring *cis*-MF molecules in the crystalline phase engage in cyclic hydrogen bonding hence coupling two carbonyl groups. As a consequence of forming hydrogen-bonded dimers, Fig. 2, the monomer C=O stretching frequency appears as a symmetric and anti-symmetric combination of frequencies and the overall dipole moment is reduced, or cancelled, because of the opposite orientation of the monomer dipoles comprising the dimers. The absence of a dipole moment associated with the dimer structures that form the basis of the crystalline lattice then accounts for the lack of a spontelectric field in the crystalline phase.

Computational investigation of the ring dimer structures of MF presented above supports this hypothesis. The computed splitting of the symmetric and anti-symmetric coupled C=O vibrations in the ring structures D1, D2, and D3 are 10, 14, and 13 cm^{-1}, respectively. On the other hand, the experimental IR spectra in Fig. 4(c) show a very broad C=O stretch band that can be decomposed into four peaks at $\approx$1719, $\approx$1710, $\approx$1703 and $\approx$1697 cm^{-1}. These peaks have to be grouped into two LO–TO pairs to represent the split symmetric and split anti-symmetric modes. An LO–TO pair of 1719 and 1703 cm^{-1} would give a midpoint at 1711 cm^{-1} and a pair of 1710 and 1697 cm^{-1}

would give one at 1704 cm^{-1}. These are consistent with the positions from Palumbo's work at 110 K ($\approx$1713 and $\approx$1707 cm^{-1}),[18] and the positions for the LO peaks from Brown's data.[19] Thus, the corresponding experimental splitting of the symmetric and anti-symmetric modes is 7 cm^{-1} which is consistent with the value of 10 cm^{-1} computed for structure D1.

Conclusions

In conclusion, a combination of measurements of spontaneous dipole orientation, IR spectroscopy and computational chemistry supports the proposal that the basis motif of the lattice in crystalline *cis*-MF is a ring dimer structure. This work would represent the first time such a combination of observations has been employed in structural identification in the solid state and shows how the spontelectric effect may be used to point the way to the identification of new structures in solid material.

Conflicts of interest

There are no conflicts to declare.

Acknowledgements

References

1 K. Kutzner, Spontaneous Polarization of condensing Carbon Monoxide and other Gases with an Electric Dipole Moment, *Thin Solid Films*, 1972, **14**, 49–61, DOI: 10.1016/0040-6090(72)90369-0.

2 R. Balog, P. Cicman, N. C. Jones and D. Field, Spontaneous Dipole Alignment in Films of N$_2$O, *Phys. Rev. Lett.*, 2009, **102**, 073003, DOI: 10.1103/PhysRevLett.102.073003.

3 D. Field, O. Plekan, A. N. Cassidy, R. Balog, N. C. Jones and J. Dunger, Spontaneous Electric Fields in Solid Films: Spontelectrics, *Int. Rev. Phys. Chem.*, 2013, **32**, 345–392, DOI: 10.1080/0144235X.2013.767109.

4 O. Plekan, A. Rosu-Finsen, A. M. Cassidy, J. Lasne, M. R. S. McCoustra and D. Field, A Review of Recent Progress in Understanding the Spontelectric State of Matter, *Eur. Phys. J. D*, 2017, **71**, 162–180, DOI: 10.1140/epjd/e2017-80048-3.

5 D. Field, Spontelectric Solids. *Proc. Roy. Soc. A*, submitted.

This journal is © the Owner Societies 2018

Phys. Chem. Chem. Phys., 2018, **20**, 29038–29044 | 29043

6 O. Plekan, A. M. Cassidy, R. Balog, N. C. Jones and D. Field, Spontaneous Electric Fields in Films of *cis*-Methyl Formate, *Phys. Chem. Chem. Phys.*, 2012, **14**, 9972–9976, DOI: 10.1039/c2cp41229b.

7 M. Roman, S. Taj, M. Gutowski, M. R. S. McCoustra, A. C. Dunn, Z. G. Keolopile, A. Rosu-Finsen, A. M. Cassidy and D. Field, Non-linear and Non-local Behaviour in Spontaneously Electrical Solids, *Phys. Chem. Chem. Phys.*, 2018, **20**, 5112–5116, DOI: 10.1039/c7cp08489g.

8 J. Lasne, A. Rosu-Finsen, A. M. Cassidy, M. R. S. McCoustra and D. Field, Spontaneously Electrical Solids in a New Light, *Phys. Chem. Chem. Phys.*, 2015, **17**, 20971–20980, DOI: 10.1039/C5CP03174E.

9 A. M. Cassidy, M. R. V. Jørgensen, A. Rosu-Finsen, J. Lasne, J. H. Jørgensen, A. Glavic, V. Lauter, B. B. Iversen, M. R. S. McCoustra and D. Field, Dipole-Oriented Molecular Solids Can Undergo a Phase Change and Still Maintain Electrical Polarization, *J. Phys. Chem. C*, 2016, **120**, 24130–24136, DOI: 10.1021/acs.jpcc.6b07296.

10 J. Lasne, A. Rosu-Finsen, A. M. Cassidy, M. R. S. McCoustra and D. Field, Spontaneous Electric Fields in Solid CO, *Phys. Chem. Chem. Phys.*, 2015, **17**, 30177–30187, DOI: 10.1039/C5CP04536C.

11 Y.-J. Chen, G. Muñoz Caro, S. Aparicio, A. Jiménez-Escobar, J. Lasne, A. Rosu-Finsen, M. R. S. McCoustra, A. M. Cassidy and D. Field, Wannier-Mott Excitons in Nanoscale Molecular Ices, *Phys. Rev. Lett.*, 2017, **119**, 157703, DOI: 10.1103/PhysRevLett.119.157703.

12 A. Dawes, R. J. Mukerji, M. P. Davies, P. D. Holtom, S. M. Webb, B. Sivaraman, S. V. Hoffmann, D. A. Shaw and N. J. Mason, Morphological Study into the Temperature Dependence of Solid Ammonia under Astrochemical Conditions using Vacuum Ultraviolet and Fourier-transform Infrared Spectroscopy, *J. Chem. Phys.*, 2007, **126**, 244711, DOI: 10.1063/1.2743426.

13 C. Bu, J. Shi, U. Raut, E. H. Mitchell and R. A. Baragiola, Effect of Microstructure on Spontaneous Polarization in Amorphous Solid Water Films, *J. Chem. Phys.*, 2015, **142**, 134702, DOI: 10.1063/1.4916322.

14 I. K. Gavra, A. N. Pilidi and A. A. Tsekouras, Spontaneous Polarization of Vapour-deposited 1-Butanol Films and its Dependence on Temperature, *J. Chem. Phys.*, 2017, **146**, 104701, DOI: 10.1063/1.4978239.

15 R. Balog, P. Cicman, D. Field, L. Feketeová, K. Hoydalsvik, N. C. Jones, T. A. Field and J.-P. Ziesel, Transmission and Trapping of Cold Electrons in Water Ice, *J. Phys. Chem. A*, 2011, **115**, 6820–6824, DOI: 10.1021/jp110475q.

16 K. Osada, K. Goushi, H. Kaji, C. Adachi, H. Ishii and Y. Noguchi, Observations of Spontaneous Orientation Polarization in Evaporated Films of Organic Light-emitting Diode Materials, *Org. Electron.*, 2018, **58**, 313–317, DOI: 10.1016/j.orgel.2018.04.026.

17 P. Friederich, V. Rodin, F. von Wrochem and W. Wenzel, Built-In Potentials Induced by Molecular Order in Amorphous Organic Thin Films, *ACS Appl. Mater. Interfaces*, 2018, **10**, 1881–1887, DOI: 10.1021/acsami.7b11762.

18 P. Modica and M. E. Palumbo, Formation of Methyl Formate after Cosmic Ion Irradiation of Icy Grain Mantles, *Astron. Astrophys.*, 2010, **519**, A22, DOI: 10.1051/0004-6361/201014101.

19 D. J. Burke, F. Puletti, P. M. Woods, S. Viti, B. Slater and W. A. Brown, Adsorption and Thermal Processing of Glycolaldehyde, Methyl Formate, and Acetic Acid on Graphite at 20 K, *J. Phys. Chem. A*, 2015, **119**, 6837–6849, DOI: 10.1021/acs.jpca.5b04010.

20 R. J. Bartlett and M. Musiał, Coupled-cluster Theory in Quantum Chemistry, *Rev. Mod. Phys.*, 2007, **79**, 291–352, DOI: 10.1103/RevModPhys.79.291.

21 T. H. Dunning, Gaussian Basis Sets for use in Correlated Molecular Calculations. I. The Atoms Boron through Neon and Hydrogen, *J. Chem. Phys.*, 1989, **90**, 1007–1023, DOI: 10.1063/1.456153.

22 R. A. Kendall, T. H. Dunning and R. J. Harrison, Electron Affinities of the First-row Atoms Revisited. Systematic Basis Sets and Wave Functions, *J. Chem. Phys.*, 1992, **96**, 6796–6806, DOI: 10.1063/1.462569.

23 R. A. Bachorz, W. Klopper and M. Gutowski, Coupled-cluster and Explicitly Correlated Perturbation-theory Calculations of the Uracil Anion, *J. Chem. Phys.*, 2007, **126**, 085101, DOI: 10.1063/1.2436890.

24 V. Barone, Anharmonic Vibrational Properties by a Fully Automated Second-order Perturbative Approach, *J. Chem. Phys.*, 2005, **122**, 014108, DOI: 10.1063/1.1824881.

25 Z. G. Keolopile, M. R. Ryder and M. Gutowski, Intermolecular Interactions between Molecules in Various Conformational States: The Dimer of Oxalic Acid, *J. Phys. Chem. A*, 2014, **118**, 7385–7391, DOI: 10.1021/jp4125638.

26 https://webbook.nist.gov/cgi/cbook.cgi?Name=methyl+formate&Units=SI&cIR=on, last accessed 03 August 2018.

27 R. F. Curl, Microwave Spectrum, Barrier to Internal Rotation, and Structure of Methyl Formate, *J. Chem. Phys.*, 1959, **30**, 1529–1536, DOI: 10.1063/1.1730232.